Int. J. Heat Mass Transfer. Vol. 31, No. 8, pp. 1655–1668, 1988
Printed in Great Britain

0017–9310/88 $3.00+0.00

Turbulence effects during evaporation of drops in clusters

J. BELLAN and K. HARSTAD
Jet Propulsion Laboratory, California Institute of Technology, 4800 Oak Grove Drive, Pasadena, CA 91109, U.S.A.

(*Received* 9 *June* 1987 *and in final form* 22 *January* 1988)

Abstract—A model of droplet evaporation in clusters and the exchange processes between the cluster and the gas phase surrounding it are presented. This model is developed for use as a subscale model in calculations of spray evaporation and combustion and thus describes only global features of cluster behavior. The gas pressure in the cluster remains constant during evaporation and as a result the volume of the cluster and the drop number density inside the cluster vary. Two turbulence models are considered. The first one describes cluster evaporation in surroundings initially devoid of turbulence and turbulence is allowed to build up with time. The second model describes cluster evaporation in surroundings where turbulence is present initially. The results obtained with these models show that turbulence enhances evaporation and is a controlling factor in the evaporation of very dense clusters; examples are shown where with the first turbulence model saturation was obtained before complete evaporation whereas the opposite was obtained with the second turbulence model. As the initial air/fuel mass ratio increases, both turbulence history and the initial relative velocity between drops and gases can control evaporation. It is shown that the evaporation time decreases with an initial increase in turbulence levels or relative velocity. When the initial air/fuel mass ratio increases further and the initial drop number density falls within the dilute regime, neither of the above parameters can control evaporation. Moreover, the evaporation time decreases with the decreasing size of the cluster for dense clusters of drops, whereas for dilute clusters of drops the size is not a controlling factor. The practical implications of these results are discussed.

1. INTRODUCTION

THE MATHEMATICAL formulation of spray combustion is extremely complicated due not only to the great number of phenomena to be described but also due to the fact that the space scales involved in these phenomena are vastly different. For example, a few of the most obvious scales are: the scale of the combustor itself, the many turbulent scales associated with turbulence build up and decay, the scale of droplet interactions and the scale of the drops themselves. These scales vary by many orders of magnitude from the largest one to the smallest one and thus it is obvious that an accurate mathematical description at all scales is impractical. Instead, a sound approach is to describe in detail the macroscale where many of the phenomena of interest to engineers involved in the design of combustors occur, and to associate and couple to this description that of phenomena occurring at scales much smaller than those of immediate interest. This second part of the formulation is called a subscale or subgrid model because the phenomena to be described occur at a scale much smaller than that of the grid size used to computationally solve the macroscale problem. By the very nature of this two-level formulation, the subscale models are more approximate than the macroscale models and lack the detail that the latter one must have in order to be useful.

The work described here pertains to a subscale model to be used for the description of spray evaporation in a combustor. Within the frame of this approximation it is intended that the gas phase in the combustor be described by the solution of the macroscale equations at certain grid points; this is an Eulerian approach. In contrast, the spray is partitioned into clusters of drops that have a size smaller than that of the grid, and each cluster is followed in its trajectory; this is a Lagrangian approach. The coupling between the two formulations is achieved through the transfer of mass, species and heat to and from the cluster. The partition of the spray into clusters as explained above is not an artifact because it is corroborated by experimental evidence [1].

What is described below is only the subgrid model uncoupled from the macroscale formulation. This means that the properties of the gas phase surrounding the cluster of drops are assumed known, and what is of interest to describe, solve for and analyze is the behavior of a cluster of drops in this given environment.

2. MODEL FORMULATION

Figure 1 shows the situation under consideration. A monodisperse collection of uniformly distributed droplets of a single-component volatile compound is immersed into gases at a higher temperature and exposed to a convective flow. As a result, heating of the drops and evaporation occurs. At each instant of time the envelope of the cluster of particles is called the surface of the cluster. The volume enclosed by the surface is called the cluster volume; it contains both drops and gas. Since the pressure is maintained constant during this process, the volume of the cluster will change with time.

The point of departure of the present model is the

NOMENCLATURE

A_c transverse area of the cluster [cm^2]
A_d cross-sectional area of a drop [cm^2]
a radius of the sphere of influence [cm]
C $-\dot{m}/[4\pi(\rho_g D)^\infty R^0]$
C_p specific heat at constant pressure [cal g^{-1} K^{-1}]
ΔC_p fitted $C_{pl}-C_{pg}$ for the saturation pressure curve [cal g^{-1} K^{-1}]
C_T constant
D diffusivity [cm^2 s^{-1}]
E_1 rate of enthalpy transfer, equation (19)
$E_{2,j}$ rates of enthalpy transfer for turbulence models 1 and 2 ($j = 1$ and 2), equations (22) and (25)
H enthalpy [cal]
H_{ref} $4R^{0^3}\rho_g^\infty L_{bn}$
$\hat{H}$ H/H_{ref}
h specific enthalpy [cal g^{-1}]
h^G enthalpy of the gases at T_{ref} [cal g^{-1}]
h^L enthalpy of the liquid at T_{ref} [cal g^{-1}]
L latent heat of evaporation [cal g^{-1}]
Le Lewis number
l_T turbulent length scale [cm]
M rate of mass transfer, equation (21)
M_{i1} rate of species i transfer, equation (20)
$M_{i2,j}$ rate of species i transfer for turbulent models 1 and 2 ($j = 1$ and 2), equations (23) and (26)
$\dot{m}$ evaporation rate, $-(1/N)\,dm_d/dt$ [g s^{-1}]
m_d mass of all drops in the cluster [g]
m_{Fv} mass of fuel vapor [g]
m_g mass of gases inside the cluster [g]
m_{ref} $4\pi\rho_g^\infty R^{0^3}$
$\hat{m}$ m/m_{ref}
N total number of drops
n drop number density [cm^{-3}]
Nu Nusselt number
p pressure [atm]
Pr Prandtl number
Re $2Ru_r/\nu_g^\infty$
Re_c $2[A_c(u_g/u_d)/\pi]^{0.5}u_d/\nu_g^\infty$
R_u^* universal gas constant [atm cm^3 mol^{-1} K^{-1}]
R_u universal gas constant [cal mol^{-1} K^{-1}]
$\tilde{R}$ radius of the cluster [cm]
$\hat{\tilde{R}}$ $\tilde{R}/R^0$
R_1 R/R^0
R drop radius [cm]
T temperature [K]
t_{ref} R^{0^2}/D^∞
T_{ref} L_{bn}/C_{pg}
t time [s]
r radial coordinate centered at a drop's center [cm]
$\tilde{r}$ radial coordinate centered at the cluster's center [cm]
R_2 a/R^0
Sh Sherwood number
u velocity [cm s^{-1}]
V volume of the cluster [cm^3]
v radial gas velocity inside the sphere of influence [cm s^{-1}]
W 'trapping factor', equation (13)
w_i molecular weight [g mol^{-1}]
y r/R^0
z r/R.

Greek symbols

α constant for the Langmuir–Knudsen evaporation law, 4π
γ w_F/w_{ag}
Γ generic function representing θ or Y_i
ε evaporation efficiency, equation (29)
θ $C_{pg}T/L_{bn}$
λ conductivity [cal cm^{-1} s^{-1} K^{-1}]
μ viscosity [g cm^{-1} s^{-1}]
ν kinematic viscosity, μ/ρ [cm^2 s^{-1}]
ρ density [g cm^{-3}]
$\hat{\rho}$ ρ/ρ_{ref}
ρ_{ref} $p^\infty w_F C_{pg}/(R_u^* L_{bn})$
σ $1-\gamma$
τ t/t_{ref}.

Subscripts

a at the edge of the sphere of influence
ag ambient gas
bn normal boiling point
c cluster
ch characteristic value
d drop
Fv fuel vapor
g gas
l liquid
r relative
s drop surface.

Superscripts

∞ in the far field of the external gas phase
0 initial value
f final: either when $R_1 = 0.04$ or when evaporation stopped.

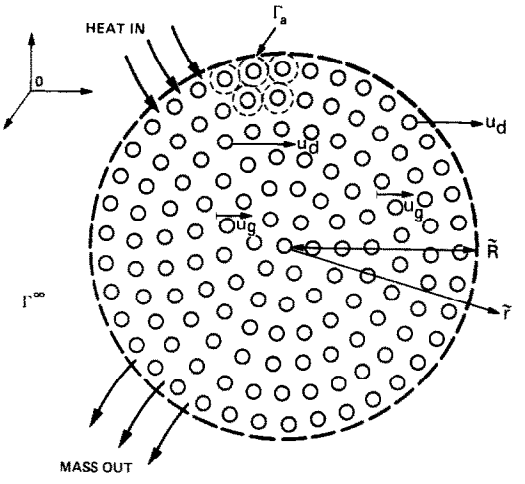

FIG. 1. Sketch of the physical situation modeled.

model of convective drop evaporation given by ref. [2]. In that model the cluster of drops was adiabatically insulated from the surroundings and the drops were moving together as a rigid entity through the flow. As a result, the gas pressure inside the cluster varied during evaporation. In contrast, in the present model there is mass and energy exchange across the surface of the cluster and drops move with respect to each other. If they move away from each other, then expansion occurs; if they move towards each other than contraction occurs. Thus, in this new configuration the drop number density becomes a dependent variable whereas the pressure becomes a constant.

The main assumptions regarding the liquid and gas phases have been described in detail elsewhere [3] and thus will not be discussed here. Similar to the study of ref. [3], in the present study each drop is considered surrounded by a sphere of influence the radius, a, of which is the half distance between the centers of two adjacent drops. The ensemble of these spheres of influence and the space between them constitutes the cluster volume. However, whereas in ref. [2] the value of the radius of the sphere of influence was a constant, here it is a variable with time. Moreover, following a previous study [2], the present formulation has three components: (a) the description of mass, species and enthalpy conservation inside the sphere of influence of each droplet; (b) the description of mass, species and enthalpy conservation in the cluster volume; and (c) the description of convective effects using differential equations expressing momentum conservation for the gases and the drops. The present description of convective effects is unchanged from ref. [2]. However, since the assumption of constant gas density inside each sphere of influence [3] is no longer valid, the solution of the convective diffusive equations inside each sphere of influence changes from its simple expression [4] to

$$\Gamma(y) = C_1 + C_2 \exp\left[C(\rho_g D)^\infty \int_y^{R_2} \frac{dy}{(\rho_g D)y^2}\right] \quad (1)$$

where C_1 and C_2 are integration constants. Now since $Le_g = 1, \rho_g D = \mu/Pr$ and using the classical expression

$$\mu = \mu_{ch}\theta_g^{0.65} \quad (2)$$

with the assumption $Pr = 0.8$ one obtains the following solution for θ_g:

$$\theta_g(y) = C_{1\theta} + C_{2\theta} \exp\left[C(\theta_g^\infty)^{0.65} \int_y^{R_2} \frac{dy}{y^2\theta_g^{0.65}}\right] \quad (3)$$

where $C_{1\theta}$ and $C_{2\theta}$ are functions of θ_{gs} and θ_{ga}. Since following the Schvab–Zeldovich approach Y_i is a linear function of θ, once θ is known so are the various Y_i's in terms of y, Y_{is} and Y_{ia}.

The derivation of equations (1)–(3) is the only novelty here in the treatment of the conservation laws inside the sphere of influence when compared with the formulation of ref. [2]. Both boundary conditions and evaporation law at the surface of the drops are the same as in ref. [2]. Moreover, the energy conservation for the liquid drops is also the same as in ref. [2] in that it considers the liquid temperature as being transient and a function of the radial position.

Note that the right-hand side of equation (3) is not analytically integrable and $\theta(y)$ can no longer be simply expressed as a function of y as in ref. [4]. This is due to the relaxation of the assumption that $\rho_g D$ is a constant. With this new formulation the equations must be solved numerically, unless some approximation is made in order to evaluate

$$Z(y) = (\theta_g^\infty)^{0.65} \int_y^{R_2} \frac{dy}{y^2\theta_g^{0.65}}. \quad (4)$$

A convenient way to evaluate $Z(y)$ is to use the weak evaporation, constant viscosity limit solution

$$\theta_g = \theta_1 + \theta_2 R_1/y \quad (5)$$

and to perform the integration analytically. This approximation preserves both the concavity of the actual temperature and its boundary values at $r = R_1$ and R_2 and therefore is expected to fit well within the present model which takes a qualitative approach to modeling rather than a quantitative approach. This approximation is also used elsewhere [5]. The qualitative approach used here is specifically concerned with global effects and does not attempt to describe accurately spacial dependence of the dependent variables. Moreover, the present formulation is qualitatively accurate only when the total number of drops, N, is much larger than unity.

To complete the description of this formulation, the following is discussed below: (1) transfer of mass, species and enthalpy from the cluster to the external gas phase; (2) the behavior of the external gas phase and transport of mass, species and enthalpy to the cluster; and (3) the conservation equations for the entire cluster.

(1) *Transfer from the cluster to the external gas phase*

The challenge here is to describe in a simple way the mass, species and energy transfer from a cluster with a moving boundary using a model that does not discriminate between the various drops and their associated surrounding gas phase in the $\tilde{r}$-direction (although nonuniformities in r are taken into account).

The global unsteady continuity equation inside the sphere of influence yields

$$\frac{\mathrm{d}}{\mathrm{d}t}\left[4\pi\int_R^a \rho_g r^2\,\mathrm{d}r\right] = 4\pi R^2(\rho_g v)_s - 4\pi R^2\frac{\mathrm{d}R}{\mathrm{d}t}\rho_{gs} - 4\pi a^2(\rho_g v)_a + 4\pi a^2\frac{\mathrm{d}a}{\mathrm{d}t}\rho_{ga}. \quad (6)$$

Since $|\mathrm{d}R/\mathrm{d}t| \ll |(v)_s|$

$$\frac{\mathrm{d}}{\mathrm{d}t}\left[4\pi\int_R^a \rho_g r^2\,\mathrm{d}r\right] = \dot{m} - \dot{m}_{loss} \quad (7)$$

where

$$\dot{m}_{loss} = 4\pi a^2\left[(\rho_g v)_a - \rho_{ga}\frac{\mathrm{d}a}{\mathrm{d}t}\right]. \quad (8)$$

Two physical limits can occur.

(a) The strictly steady situation where

$$4\pi R^2(\rho_g v)_s = 4\pi a^2(\rho_g v)_a \quad (9)$$

and according to equation (8) one obtains

$$\dot{m}_{loss} = \dot{m} - 4\pi a^2\frac{\mathrm{d}a}{\mathrm{d}t}\rho_{ga}. \quad (10)$$

In this limit maximum new vapor passes through the sphere of influence and escapes to ambient. Then

$$(v)_a = \frac{\dot{m}}{4\pi a^2\rho_{ga}}.$$

(b) The limit where all new vapor is trapped into the sphere of influence as its surface moves. Then

$$\dot{m}_{loss} = 0 \quad (11)$$

and

$$(v)_a = \frac{\mathrm{d}a}{\mathrm{d}t}. \quad (12)$$

The physical reality is somewhat in between these two limits. We thus define a 'trapping factor'

$$W = m_g/(m_g + m_d) \quad (13)$$

and model

$$(v)_a = (1-W)\frac{\dot{m}}{4\pi a^2\rho_{ga}} + W\frac{\mathrm{d}a}{\mathrm{d}t}. \quad (14)$$

Thus this expression gives the velocity of the gases at the edge of the sphere of influence in the general case and also satisfies the above two limits because: (i) in the dilute limit $m_d \ll m_g$ and $W \to 1$; (ii) in the strong evaporation, strictly steady, limit $W \to 0$ because $m_g \ll m_d$.

Since in this model there is no distinction between the surface of the cluster and surface of the spheres of influence the mass and enthalpy loss from the cluster are respectively $N\dot{m}_{loss}$ and $N\dot{m}_{loss}h_{ga}$. The effect of the convective flow on drop evaporation is contained in $\dot{m}$ which is the solution of the purely diffusive evaporation case multiplied by a corrective factor as described in ref. [2].

(2) *The behavior of the gas phase external to the cluster and transport to the cluster*

In order to be consistent with the treatment of convective drop evaporation of ref. [2], which is still preserved here, where convective effects are considered as a correction to diffusive evaporation, the external gas phase is first considered to have a purely diffusive behavior and Y_i and θ satisfy

$$\frac{1}{\tilde{r}^2}\frac{\mathrm{d}}{\mathrm{d}\tilde{r}}\left(\tilde{r}^2\frac{\mathrm{d}\Gamma}{\mathrm{d}\tilde{r}}\right) = 0. \quad (15)$$

The solution of this equation is

$$\Gamma(\tilde{r}) = (\Gamma_\alpha - \Gamma_a^\infty)\frac{\tilde{R}}{\tilde{r}} + \Gamma^\infty \quad (16)$$

assuming continuity for Γ at $\tilde{r} = \tilde{R}$. Thus

$$-\lambda_g^\infty\left.\frac{\mathrm{d}\theta}{\mathrm{d}\tilde{r}}\right|_{\tilde{R}} = \lambda_g^\infty(\theta_g^\infty - \theta_{ga})\frac{1}{\tilde{R}} \quad (17)$$

$$-\rho_g D^\infty\left.\frac{\mathrm{d}Y_i}{\mathrm{d}\tilde{r}}\right|_{\tilde{R}} = \rho_g D^\infty(Y_i^\infty - Y_{ia})\frac{1}{\tilde{R}}. \quad (18)$$

Similarly to the description of convective effects of ref. [2], these are seen as a contribution both from the individual droplet and the entire cluster.

The contribution to heat transfer from the individual drops is due to the cluster 'porosity'. Consistent with the present homogeneous description for the cluster in the $\tilde{r}$-direction this contribution for heat, species and mass is modeled as

$$E_1 = (\rho_g^\infty h_g^\infty - \rho_{ga}h_{ga})u_r A_c \quad (19)$$

$$M_{i1} = (\rho_g^\infty Y_i^\infty - \rho_{ga}Y_{ia})u_r A_c \quad (20)$$

$$M = (\rho_g^\infty - \rho_{ga})u_r A_c. \quad (21)$$

The heat transfer to the entire cluster is highly dependent upon turbulent transfer between the surroundings and the cluster. Because of this, it is very important to understand how the history of turbulence with respect to that of evaporation influences the behavior of the cluster. For this reason, two turbulence models are considered and compared here. Since in our calculations the coordinate system is fixed with the state of the gases at $t = 0$, $u_g^0 = 0$ and thus in the first model the drops do not act initially as an entity, but rather as individuals and turbulence builds up with time if the cluster 'porosity' diminishes significantly. In this model the rate of heat and species

transfer integrated over the entire surface of the cluster is

$$E_{2,1} = 4\pi \frac{\lambda_g^\infty}{C_{pg}} L_{bn} Nu_c \frac{u_g}{u_d} \tilde{R}(\theta_g^\infty - \theta_{ga}) \quad (22)$$

$$M_{i2,1} = 4\pi(\rho_g D)^\infty Sh_c \frac{u_g}{u_d} \tilde{R}(Y_i^\infty - Y_{ia}). \quad (23)$$

Under the assumption of similarity between heat and mass transfer $Sh_c = Nu_c$. In the computations further presented here the value of Nu_c was taken to be that for flows around a sphere up through the turbulent range [6]

$$Nu_c = 1 + 0.19 Pr^{1/3} Re_c^{3/5} \quad (24)$$

where Re_c is based upon the length scale $[A_c(u_g/u_d)/\pi]^{0.5}$ and velocity u_d [2]. The quantity $A_c(u_g/u_d)$ is an effective cluster area which was found to be important in determining the drag due to the surface force on the cluster as a result of its motion through the gas [2]. The ratio u_g/u_d is in fact equal to the non-slip displacement gas flow divided by the total gas flux.

The second turbulence model used here is different from the first one in that the turbulent part of the Nusselt number is changed in such a manner as to be consistent with the cluster surroundings being initially turbulent. This is done by making the turbulent contribution of Nu_c proportional to u_d rather than u_g. In this second formulation

$$E_{2,2} = 4\pi \frac{\lambda_g^\infty}{c_{pg}} L_{bn} \left(\frac{u_g}{u_d} + \frac{C_T}{2} Pr\, Re_T \right) \tilde{R}(\theta_g^\infty - \theta_{ga}) \quad (25)$$

$$M_{i2,2} = 4\pi(\rho_g D)^\infty \left(\frac{u_g}{u_d} + \frac{C_T}{2} Pr\, Re_T \right) \tilde{R}(Y_i^\infty - Y_{ia}) \quad (26)$$

where

$$Re_T = 2\rho_{ga} \tilde{R} u_d / \mu_g^\infty \quad (27)$$

$$C_T \equiv l_T / \tilde{R} \quad (28)$$

and C_T is a constant.

(3) *The conservation equations for the entire cluster*

Under the quasi-steady assumption these equations are as follows.

(a) *Conservation of total mass of liquid fuel.* This states that the mass of liquid fuel at time t is equal to the initial fuel mass minus the mass evaporated from the drops. Once nondimensionalized the equation becomes

$$\varepsilon = 1 - R_1^3. \quad (29)$$

(b) *Conservation of total gaseous mass inside the cluster.* The gaseous mass at time t is the sum of the initial gas mass, the mass evaporated from the fuel, and the mass entering the cluster of drops minus the mass loss from the cluster to the surroundings. This is expressed as

$$\frac{dm_g}{dt} - N\dot{m} - N\dot{m}_{loss} + (\rho_g - \rho_{ga}^\infty) u_r A_c \quad (30)$$

where

$$m_g = N \int_R^a 4\pi r^2 \rho_g(r)\, dr + \left(V - \frac{4\pi a^3}{3} N \right) \rho_{ga} \quad (31)$$

and m_{loss} is given by equations (8) and (14). To calculate the density integral, the equation of state is invoked to obtain

$$\int_R^a \rho_g(r) r^2\, dr = \frac{p^\infty w_F C_{pg}}{R_u^* L_{bn}} R^{0^3} \int_{R_1}^{R_2} \frac{y^2\, dy}{\theta_g(\sigma Y_{Fv} + \gamma)} \quad (32)$$

where

$$Y_{Fv} + Y_{ag} = 1 \quad (33)$$

was used. The form of equation (31) becomes integrable when θ_g is given by the approximation of equation (5) and Y_{Fv} is obtained in a similar way. In this manner m_g can be approximated by an analytic, non-linear function G

$$m_g = G(R_2, R_1, n, \theta_{ga}, \theta_{gs}, Y_{Fva}, Y_{Fvs}). \quad (34)$$

(c) *Conservation of fuel vapor mass inside the cluster.* The time change of fuel vapor mass inside the cluster is due to mass addition from the evaporated drops, mass addition from fuel transported from the external gas phase to the cluster and mass depletion due to fuel escaping from the cluster to the external gas phase. This is expressed by

$$\frac{dm_{Fv}}{dt} = N\dot{m} + M_{F1} + M_{F2,j} - N\dot{m}_{loss} Y_{Fva} \quad (35)$$

where

$$m_{Fv} = N \int_R^a \rho_g Y_{Fv} 4\pi r^2\, dr + \left(V - \frac{4\pi a^3}{3} N \right) \rho_{ga} Y_{Fva} \quad (36)$$

and $\dot{m}_{loss}$, M_{F1} and $M_{F2,j}$ are given, respectively, by equations (8), (14), (20), and (23) or (26). Now

$$\int_R^a \rho_g Y_{Fv} r^2\, dr = \frac{p^\infty w_F R^{0^3} C_{pg}}{R_u^* L_{bn}} \int_{R_1}^{R_2} \frac{y^2 Y_{Fv}\, dy}{\theta_g(\sigma Y_{Fv} + \gamma)} \quad (37)$$

and using again the approximation of equation (5) we can approximate m_{Fv} by an analytic, non-linear function F

$$m_{Fv} = F(R_2, R_1, n, \theta_{ga}, \theta_{gs}, Y_{Fvs}, Y_{Fva}). \quad (38)$$

(d) *Conservation of total enthalpy inside the cluster.* The change of total enthalpy inside the cluster is due to enthalpy being transferred from the external gas phase to the cluster and enthalpy escaping with the gaseous outflow from the cluster. In all the calculations made here it was assumed that initially the

temperature of the external gas phase is much higher than that of the gases inside the cluster, so that heat conduction from the gases inside the cluster to the external gas phase is excluded. Thus the enthalpy equation is

$$\frac{\mathrm{d}H}{\mathrm{d}t} = E_1 + E_{2,j} - N\dot{m}_{\mathrm{loss}} h_{\mathrm{ga}} \tag{39}$$

where $\dot{m}_{\mathrm{loss}}$, E_1 and $E_{2,j}$ are respectively given by equations (8), (14), (19) and (22) or (25) and

$$H = N\int_0^R 4\pi r^2 h_{\mathrm{l}}\rho_{\mathrm{l}}\,\mathrm{d}r + N\int_R^a 4\pi r^2 h_{\mathrm{g}}\rho_{\mathrm{g}}\,\mathrm{d}r + \left(V - \frac{4\pi a^3}{3}N\right)h_{\mathrm{ga}}\rho_{\mathrm{ga}} \tag{40}$$

with

$$h_{\mathrm{g}} = h^{\mathrm{G}} + C_{p\mathrm{g}}(T_{\mathrm{g}} - T_{\mathrm{ref}}) \tag{41}$$

$$h_{\mathrm{l}} = h^{\mathrm{L}} + C_{p\mathrm{l}}(T_{\mathrm{l}} - T_{\mathrm{ref}}) \tag{42}$$

$$L \equiv h_{\mathrm{g}} - h_{\mathrm{l}}. \tag{43}$$

With the above definitions H becomes

$$H = N\rho_{\mathrm{l}}4\pi\left[\frac{R^3}{3}h^{\mathrm{L}} + C_{p\mathrm{l}}\int_0^R (T_{\mathrm{l}} - T_{\mathrm{ref}})r^2\,\mathrm{d}r\right] + 4\pi N\left[(h^{\mathrm{G}} - C_{p\mathrm{g}}T_{\mathrm{ref}})\int_R^a \rho_{\mathrm{g}}r^2\,\mathrm{d}r + C_{p\mathrm{g}}\int_R^a r^2 T_{\mathrm{g}}\rho_{\mathrm{g}}\,\mathrm{d}r\right] + \left(V - \frac{4\pi a^3}{3}N\right)[h^{\mathrm{G}} + C_{p\mathrm{g}}(T_{\mathrm{ga}} - T_{\mathrm{ref}})]\rho_{\mathrm{ga}}. \tag{44}$$

The first integral in equation (44) can be easily performed since, as it will be explained in the next section, $T_{\mathrm{l}}(r)$ is solved as a series solution from the energy conservation equation inside each drop, and the two last integrals in equation (44) are calculated using the approximation previously described to calculate $\theta_{\mathrm{g}}(y)$ from equation (3). Thus, one approximates H by an analytic, non-linear function

$$H = \mathscr{H}(R_2, R_{\mathrm{l}}, n, \theta_{\mathrm{ga}}, \theta_{\mathrm{gs}}, Y_{\mathrm{Fva}}, Y_{\mathrm{Fvs}}). \tag{45}$$

One can eliminate n as a dependent variable from the above equation by noting that for tightly packed spheres [7]

$$n = 0.74\frac{3}{4\pi a^3}. \tag{46}$$

Thus the dependent variables which are the unknowns in this problem are: ε, R_{l}, R_2, θ_{gs}, θ_{ga}, Y_{Fvs}, Y_{Fva}, C, u_{r}, u_{d}. The equations which are solved to find the solution for these ten variables are given in non-dimensional form in the Appendix.

3. NUMERICAL PROCEDURES

The integrated drop energy equation is

$$\frac{\mathrm{d}}{\mathrm{d}t}\left(4\pi\rho_{\mathrm{l}}\int_0^R h_{\mathrm{l}}r^2\,\mathrm{d}r\right) = 4\pi R^2\lambda_{\mathrm{l}}\frac{\partial T_{\mathrm{l}}}{\partial r}\bigg|_{r\to R} - \dot{m}h_{\mathrm{l}}\bigg|_{r=R}. \tag{47}$$

The temperature distribution $T_{\mathrm{l}}(r)$ in the drop is obtained by solution of the drop heat conduction equation by means of expansion in a small parameter inversely proportional to λ_{l} [3]. This results in the formation of two differential equations in time for functional parameters, which in conjunction with the surface gradient expression (A7) in the Appendix, determine the temperature distribution; the particulars are given in ref. [3]. The above equation is combined with the global energy equation, equation (39), to obtain an enthalpy equation for the gas phase

$$\frac{\mathrm{d}}{\mathrm{d}t}\left[(4\pi R^{0^3}\rho_{\mathrm{ref}})Nh + \left(V - \frac{4\pi}{3}a^3N\right)\rho_{\mathrm{ga}}\theta_{\mathrm{ga}}\right] = N\dot{m}\left[\frac{\theta_{\mathrm{gs}} - \theta_{\mathrm{ga}}\exp(CZ(R_{\mathrm{l}}))}{1 - \exp(CZ(R_{\mathrm{l}}))}\right] + \frac{E_{2,j}}{L_{\mathrm{bn}}} + (\rho_{\mathrm{g}}^{\infty}\theta_{\mathrm{g}}^{\infty} - \rho_{\mathrm{ga}}\theta_{\mathrm{ga}})u_{\mathrm{r}}A_{\mathrm{c}} - N\theta_{\mathrm{ga}}\dot{m}_{\mathrm{loss}} \tag{48}$$

where the function h is given by equation (A3).

Since there is a linear relationship between the Y_i's and temperature, equations (30), (35) and (39) are not independent. The following holds

$$Y_{\mathrm{Fv}}^{\infty}(\theta_{\mathrm{ga}} - \theta_{\mathrm{gs}}) = Y_{\mathrm{Fvs}}\theta_{\mathrm{ga}} - Y_{\mathrm{Fva}}\theta_{\mathrm{gs}} - (Y_{\mathrm{Fvs}} - Y_{\mathrm{Fva}})\theta_{\mathrm{g}}^{\infty}. \tag{49}$$

Variables and determining equations are as follows: θ_{gs} (or θ_{ls}) is obtained from the drop heat conduction equation, m_{g} from equation (30), h from equation (48), Y_{Fvs} and Y_{Fva} from equations (49) and (A8), C from equation (A5), R_{l} from equation (A6), u_{d} from equation (A9), and u_{r} from equation (A10). Both m_{g} and h are known functions of the dependent variables; m_{g} (or function g) is considered as determining θ_{ga} and h determines R_2. (These functions vary most strongly with this particular variable selection.) The variables C, Y_{Fvs}, Y_{Fva}, R_2 and θ_{ga} are governed by a non-linear set of algebraic equations; the other variables are determined directly from differential equations.

Eliminating Y_{Fva} from equations (49) and (A8) results in an equation relating Y_{Fvs} to C. The evaporation equation, equation (A5), also relates these two variables. These two equations are iterated in an inner loop for the variables, considering all other variables fixed. In an outer loop, functions g and h are iterated for R_2 and θ_{ga}. This nested loop procedure allows for a relatively efficient solution of the algebraic equations at each time step of the differential equation integration. The differential equations are integrated using a standard ODE integrator, GEAR, with a local error tolerance of 10^{-4}.

The model equations depend on terms proportional

to dR_2/dt. Since R_2 is formed algebraically, this derivative needs to be estimated. The procedure for calculating this derivative is as follows. Define

$$h' \equiv h + \frac{1-0.74}{3\times 0.74}\hat{\rho}_{ga}\theta_{ga};$$

this is the unknown in equation (48). On the other hand $h' \equiv R_2^3 J$, where J is a relatively weak varying function. Thus

$$3R_2^2\frac{dR_2}{dt} = \left(\frac{dh'}{dt} - R_2^3\frac{dJ}{dt}\right)\Big/ J$$

where dh'/dt is known and dJ/dt is approximated by a third-order backward finite difference.

4. RESULTS AND DISCUSSION

The results presented below were obtained from calculations performed for liquid n-decane drops evaporating in initially unvitiated air. The thermophysical constants for n-decane that were used here are the same as those of ref. [3]. The interest here is on how turbulence can affect evaporation of drops in clusters and the behavior of the cluster as an entity.

Figure 2 shows a non-dimensional evaporation time vs the initial air/fuel mass ratio for three situations. The baseline case is that of the first turbulence model and $u_r^0 = 500$ cm s^{-1}. The two cases are chosen such as to study the influence upon evaporation of both the initial relative velocity and the turbulence history. The plots show that in the very dense spray regime the initial relative velocity is not a good control parameter. However, by changing the history of turbulence with respect to that of evaporation, one can obtain now complete evaporation in situations where the gases in the cluster saturated before complete evaporation when the other turbulence model was used. The reason for this is that as the drops heat up, the gases cool off; if the exchange of mass and heat between the cluster and the surroundings is poor, the gases in the cluster will saturate and the drops will eventually be at the same temperature as the gases thereby stopping evaporation. On the other hand if fresh gases and energy can be brought inside the cluster from the surroundings, evaporation will proceed. These processes are most important during the initial part of evaporation, when the rate of mass loss from the drop is high. If turbulence is not present at that time, evaporation will eventually stop as shown by the baseline case; an increase in the initial relative velocity does not affect the outcome. Since turbulence model 2 portrays a case where turbulence is present initially, the exchange of mass and heat between the gases inside and outside the cluster occurs at the appropriate time, and evaporation can be completed.

For smaller ϕ^0, there is a regime where both the turbulence history and u_r^0 can control evaporation. By increasing u_r^0 one can now obtain complete evaporation before saturation with the same turbulence history; by keeping u_r^0 constant and changing the turbulence history one obtains the same outcome, however, the evaporation time is now considerably shorter.

When ϕ^0 increases even further, and the regime of the slightly rich and further that of the lean mixtures is encountered, neither turbulence nor the initial relative velocity are good control parameters. In fact as n^0 decreases to a few drops-cm^{-3}, any one of the three models gives exactly the same result and all three models reach the same asymptote. The reason for this is that as the initial density of drops in the cluster decreases, the interstitial gas between the drops cools less during evaporation, and mass and heat transfer from the surroundings plays a decreasingly important role. In the same manner, as the initial density of drops in the cluster decreases, the drops reach the asymptote corresponding to the limit of the convective evaporation of 1 drop-cm^{-3} [2].

These conclusions are substantiated by the results plotted in Figs. 3–5. Depicted in Fig. 3 are both the gas temperature drop and the gas density rise as a function of ϕ^0. For very lean mixtures and dilute clusters there is no temperature drop since the heat going to the drops to support evaporation is minimal compared to the total heat available in the gases of the cluster. As ϕ^0 decreases and the regime of rich mixtures is reached, a temperature drop and a corresponding density rise are encountered. With a further decrease in ϕ^0 one can observe the influence of turbulent heat transfer from the surroundings in keeping the temperature at a level where it can support evaporation. In contrast, when turbulence is not present initially and instead develops with time the temperature drop is more substantial and eventually reaches the point where it can no longer support evaporation.

The reason that the initial history of turbulence is so important in controlling evaporation is illustrated in Fig. 4. Not only is $\dot{m}$ largest when the drops are larger [2], but also the loss fraction is largest initially. By the time $R_1 = 0.5$, the loss fraction is negligible. The oscillations in $\dot{m}_{loss}/\dot{m}$ observed in the figure inset may be due to the inaccurate numerical evaluation of da/dt using a two step backward scheme. Since these oscillations occur in a region where $|\dot{m}_{loss}/\dot{m}| \ll 1$, no further effort has been made to improve the accuracy.

The loss fraction accounts only for the mass lost from the system as a result of the motion of the cluster surface, but does not account for the gain that occurs when mass is brought into the cluster by turbulent transfer from the surroundings. As a result, its value as a diagnostic is limited to indicating the relative importance of gaseous mass lost from the cluster to gaseous mass gained inside the cluster through evaporation. In contrast, the global mass conservation equation for the cluster does account appropriately for mass addition due to turbulent transport.

The variation of the final position of the cluster surface with respect to its initial position is shown vs ϕ^0 in Fig. 5. As expected, for lean mixtures and dilute

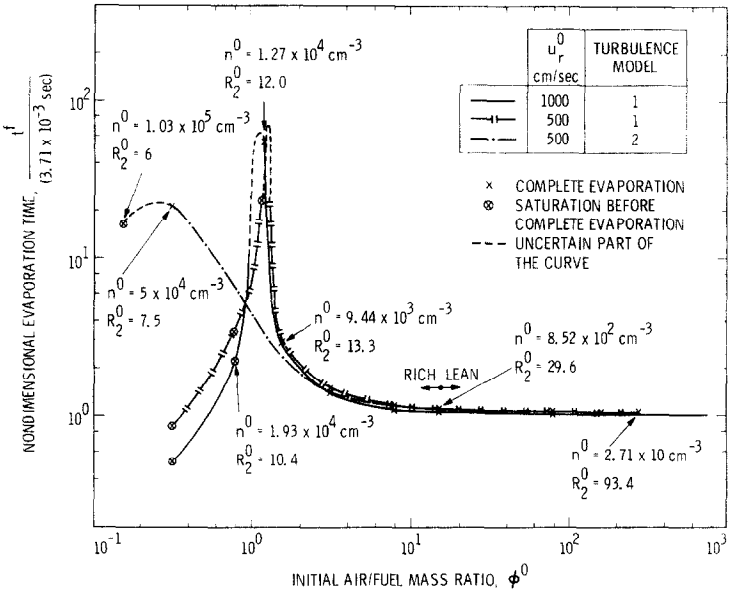

FIG. 2. Variation of a non-dimensional evaporation time with the initial air/fuel mass ratio: $T_{ga}^0 = 1000$ K, $T_{gs}^0 = 350$ K, $Y_{Fva}^0 = 0$, $\tilde{R}^0 = 10$ cm, $R^0 = 2 \times 10^{-3}$ cm.

sprays, when there is not much gaseous mass added through evaporation, the cluster maintains its original size. As ϕ^0 decreases the cluster shrinks in size due to internal cooling. However, this shrinkage is smaller for turbulence model 2, as the final temperature was also observed to be higher. This contraction is consistent with the observed decrease in pressure inside the cluster when evaporation occurred in a cluster that was adiabatically insulated from the surroundings [2]. This pressure drop was larger with decreasing ϕ^0, which means that despite the very large increase in density in the very rich cases, the cooling effect was dominant.

If the mass lost from the cluster is integrated in time, converted into a volume by dividing by ρ_g^∞, and finally nondimensionalized by the initial volume of the cluster one finds that at fixed R_1 this value is larger for smaller ϕ^0 and at fixed ϕ^0 it is larger for turbulence model 1. When this value is added, at fixed R_1, to the non-dimensionalized cluster volume, one finds that for a given ϕ^0 the sum is larger for turbulent model 2. In all cases this sum is consistently smaller than unity and increases with the value of ϕ^0 approaching unity for large values of ϕ^0. These results confirm the fact that even when one accounts for the mass escaping from the cluster, contraction due to cooling of the gases occurs. With turbulence model 1 more of the gas escapes to the surroundings and with turbulence model 2 less of a contraction occurs.

It is worth mentioning that the differences observed between the behavior of the clusters when the two turbulence models are considered is not due to the

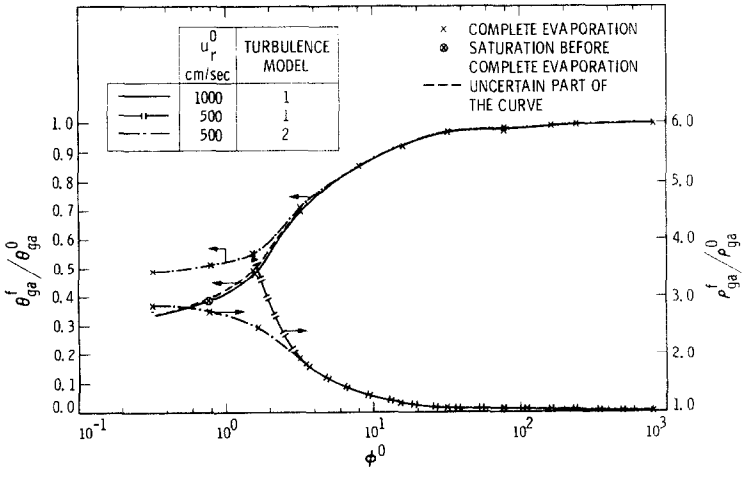

FIG. 3. Variation of $\theta_{ga}^f/\theta_{ga}^0$ and ρ_{ga}^f/ρ_{ga}^0 with the initial air/fuel mass ratio: $T_{ga}^0 = 1000$ K, $T_{gs}^0 = 350$ K, $Y_{Fva}^0 = 0$, $\tilde{R}^0 = 10$ cm, $R^0 = 2 \times 10^{-3}$ cm.

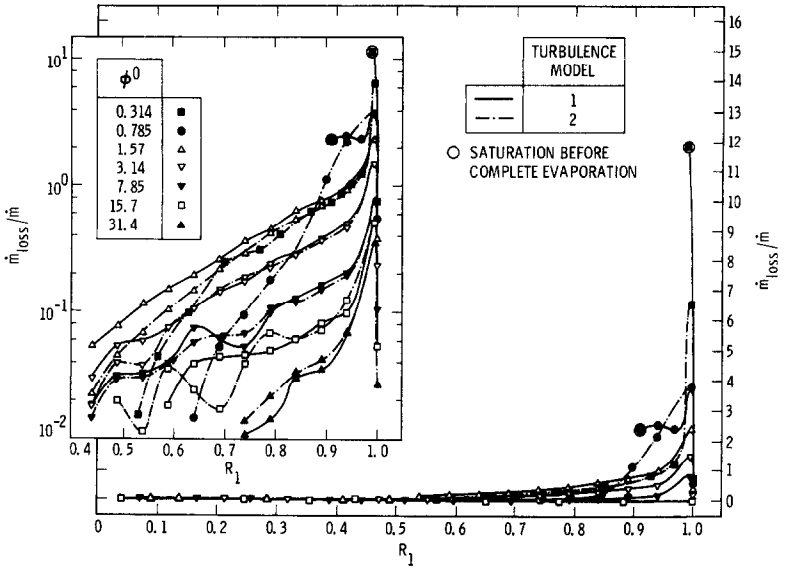

FIG. 4. Loss fraction vs R_1 for various initial air/fuel mass ratios: $T^0_{ga} = 1000$ K, $T^0_{gs} = 350$ K, $Y^0_{Fva} = 0$, $\tilde{R}^0 = 10$ cm, $R^0 = 2 \times 10^{-3}$ cm, $u^0_r = 500$ cm s^{-1}.

fact that the drops evaporate in different regimes [2] (diffusive, convective–diffusive or convective) but rather due to the different exchange processes between the clusters and their surroundings. Figure 5 illustrates the fact that the initial penetration distance, which indicates the evaporation regime [2], varies only with u^0_r and ϕ^0 and not with the turbulence model. At fixed ϕ^0, as R_1 decreases the penetration ratios continue to be extremely close for the two turbulence models.

The effect of varying the cluster size can be seen in Fig. 6 where a non-dimensional evaporation time is plotted vs the initial size of the cluster for both turbulence models. For a stoichiometric mixture neither the initial size of the cluster nor the turbulence model influence very much the evaporation time; however, there is a slight tendency to a larger evaporation time with increased initial size. This effect is very substantial for rich mixtures and is observed for both turbulence models. There are several reasons for this. First, since u^0_r is fixed, as the cluster becomes smaller, the initial penetration ratio is larger and the drops evaporate in a regime which changes from diffusive to predominantly convective thus reducing the evaporation time. This is illustrated in Fig. 7 where $(L_p/\tilde{R})^0$ is plotted vs $\tilde{R}^0$. In contrast, for stoichiometric mixtures the evaporation regime is convective–diffusive to convective and as it has been pointed out previously [2], convective effects always dominate diffusive effects thus determining the evaporation time. Second, although at fixed ϕ^0, n^0 is the same for all sizes of clusters, N decreases with $\tilde{R}^0$. This leads to a more pronounced interaction with the surroundings and thus faster evaporation.

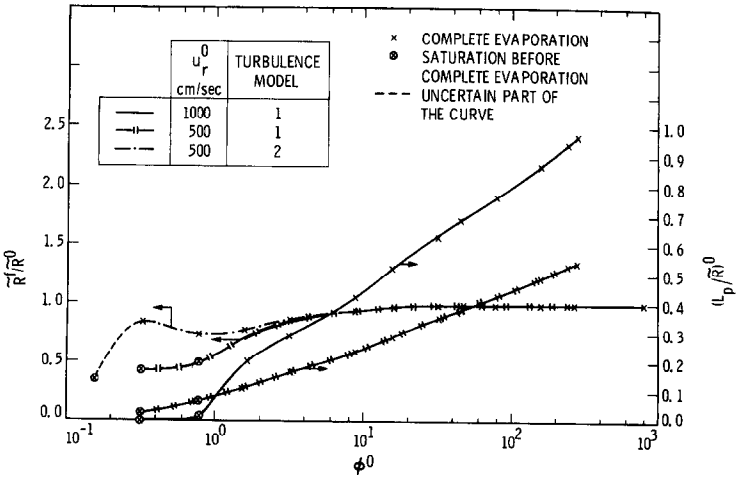

FIG. 5. Initial penetration ratio and final position of the cluster surface vs the initial air/fuel mass ratio: $T^0_{ga} = 1000$ K, $T^0_{gs} = 350$ K, $Y^0_{Fva} = 0$, $\tilde{R}^0 = 10$ cm, $R^0 = 2 \times 10^{-3}$ cm.

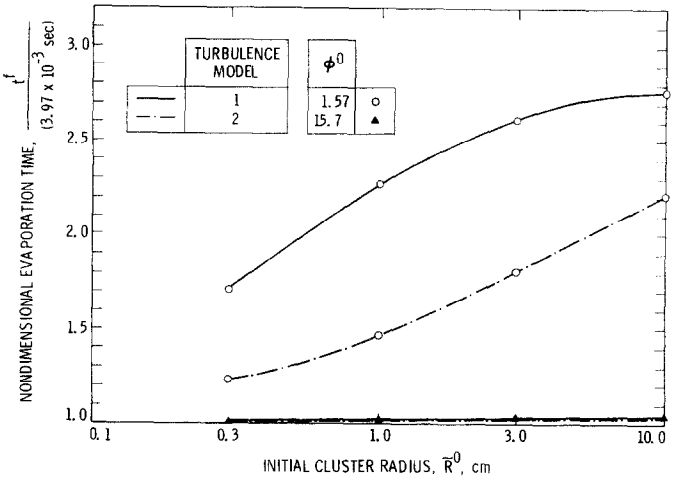

FIG. 6. Variation of a non-dimensional evaporation time with the initial radius of the cluster: $T^0_{ga} = 1000$ K, $T^0_{gs} = 350$ K, $Y^0_{Fva} = 0$, $R^0 = 2 \times 10^{-3}$ cm, $u^0_r = 500$ cm s^{-1}.

The total effect upon the final cluster size is presented in Fig. 7. In all cases larger clusters contract more, relative to their initial size, than do smaller clusters due again to the cooling effect discussed above. A smaller number of drops in a cluster results in less cooling of the gas phase at complete evaporation and faster evaporation.

Similarly to the discussion pertinent to Fig. 2, turbulence model 2 predicts shorter evaporation times for dense clusters and the same evaporation time for dilute clusters as does turbulence model 1. The trends regarding $\tilde{R}^f/\hat{R}^0$ are also similar.

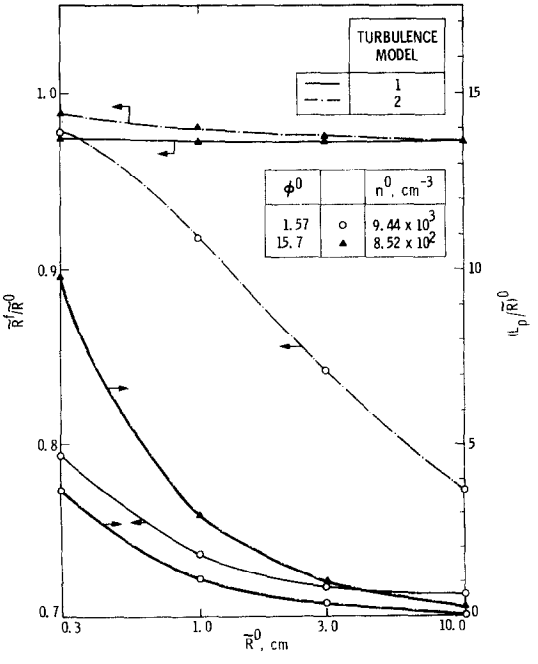

FIG. 7. Initial penetration ratio and final position of the cluster surface vs the initial radius of the cluster: $T^0_{ga} = 1000$ K, $T^0_{gs} = 350$ K, $Y^0_{Fva} = 0$, $R^0 = 2 \times 10^{-3}$ cm, $u^0_r = 500$ cm s^{-1}.

In order to gain a better understanding about the behavior of the cluster we display in Figs. 8 and 9 the history of $\tilde{R}/\tilde{R}^0$. Since there is a certain uncertainty about the time taken to evaporate, and since it depends strongly upon the evaporation model, in order to partially eliminate this uncertainty, the plots are made vs R_1. Figure 8 represents the situation for a rich mixture, whereas Fig. 9 represents the situation for a stoichiometric mixture. The striking feature in Fig. 8 is the initial drop in $\tilde{R}/\tilde{R}^0$ which, as discussed above, is due to the cooling of the gas phase and the continual heating of the drops. Following this decrease in $\tilde{R}/\tilde{R}^0$, a minimum in this value is reached, after which there ensues a recovery. This recovery is due to the unvitiated (by fuel) hot gas brought in through turbulent transport from the gas phase surrounding the cluster. As expected, turbulence model 2 offers more possibilities for recovery. As the cluster is smaller and the number of drops decreases, there is less of a drop in $\tilde{R}/\tilde{R}^0$, the minimum $\tilde{R}/\tilde{R}^0$ occurs earlier with respect to R_1 and the final value of $\tilde{R}/\tilde{R}^0$ is closer to unity. Figure 9 shows that in contrast to the rich mixtures, for stoichiometric mixtures there is no minimum in $\tilde{R}/\tilde{R}^0$; the size of the cluster continuously decreases with R_1. However, there is less of a cluster shrinkage due to the fact that there is less mass in the cluster, less cooling and less mass loss.

The practical implications of these results with regard to optimization of evaporation is straightforward. Turbulence should be induced in the gas in which the spray is injected prior to or at the same time as injection. Turbulence can help to evaporate the drops of the spray through two processes. First it can break the spray into clusters and the smaller the cluster, the shorter the evaporation time. Second, it brings in unvitiated (by fuel) hot gas from the surrounding of the clusters thereby enhancing and supporting evaporation. Moreover, the results show that evaporation of drops in dense clusters can be con-

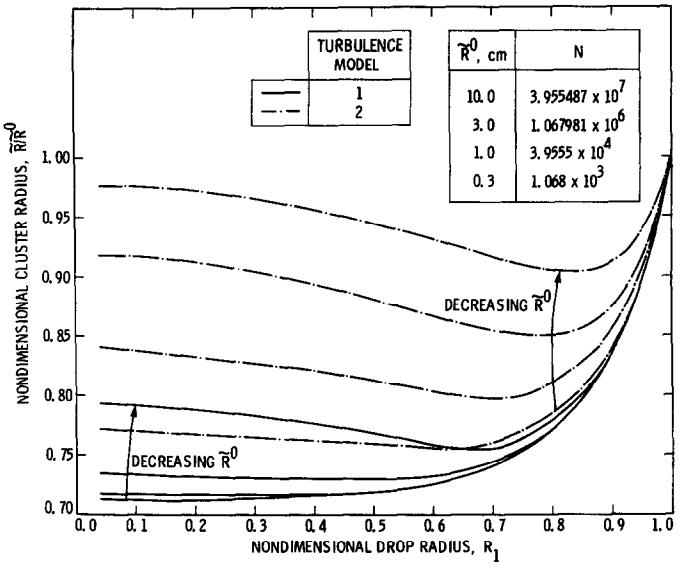

FIG. 8. Variation of the residual cluster radius with R_1 for different initial cluster radii for a dense cluster of drops: $T^0_{ga} = 1000$ K, $T^0_{gs} = 350$ K, $Y^0_{Fva} = 0$, $R^0 = 2 \times 10^{-3}$ cm, $u^0_r = 500$ cm s^{-1}, $\phi^0 = 1.57$ ($n^0 = 9.44 \times 10^3$ cm^{-3}; $R^0_2 = 13.3$).

trolled whereas when they are in a dilute configuration it cannot. This means that evaporation control should be envisaged near the injector in order to be truly effective, rather than further along the combustor.

5. SUMMARY AND CONCLUSIONS

The model presented above is one example of subgrid models that are needed to describe spray evaporation and combustion. As such, the predictions of the model pertain to the global behavior of clusters of drops rather than the detail of the behavior of each drop in the cluster and the difference in behavior between the drops belonging to the same cluster.

Despite the simplicity of the turbulence models used herein there are many important aspects that have been elucidated by the results obtained with the two models. First, in contrast to dilute clusters of drops, the evaporation of very dense clusters of drops is greatly affected by the initial level of turbulence in the surrounding gas. Not only is the evaporation time affected but also it is shown that by having turbulence initially present rather than letting it build with time, one can obtain complete evaporation before saturation in situations where otherwise saturation was obtained before complete evaporation. Thus, for dense sprays the transfer processes between the gases in the cluster and the surroundings are crucial in deter-

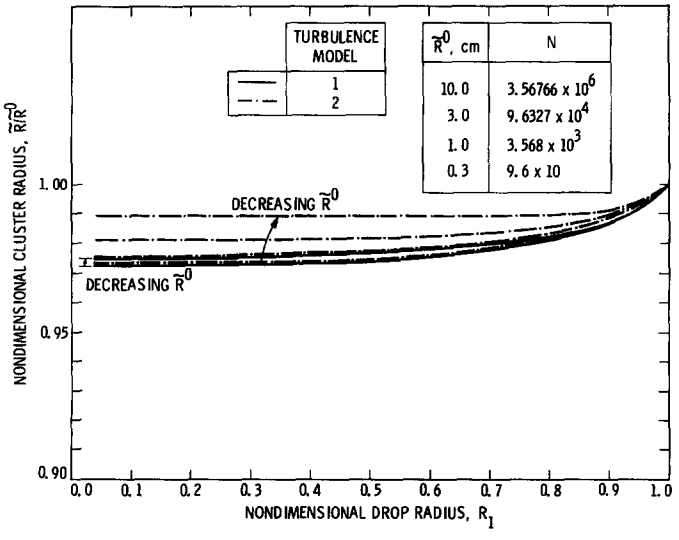

FIG. 9. Variation of the residual cluster radius with R_1 for different initial cluster radii for a dilute cluster of drops: $T^0_{ga} = 1000$ K, $T^0_{gs} = 350$ K, $Y^0_{Fva} = 0$, $R^0 = 2 \times 10^{-3}$ cm, $u^0_r = 500$ cm s^{-1}, $\phi^0 = 15.7$ ($n^0 = 8.52 \times 10^2$ cm^{-3}; $R^0_2 = 29.6$).

mining the outcome of evaporation. Between these regimes of very dense and dilute clusters there exists a regime where both the history of turbulence and the initial relative velocity between drops and gases can be important control parameters.

Furthermore, the results show that the evaporation time of a dilute cluster cannot be decreased by reducing its initial size while keeping the initial air/fuel mass ratio constant. In contrast, for dense clusters, the evaporation time decreases with the initial size of the cluster at the same initial air/fuel mass ratio. Moreover, by having turbulence present initially, rather than letting it build up, the evaporation time of the cluster can be further decreased.

Thus gas phase turbulence can be important in reducing the evaporation time in two ways. First, turbulence breaks up the spray in small size clusters right at the exit of the atomizer, where the spray is dense. Second, turbulence acts as a vehicle for transporting mass, species and heat to the cluster, thus supporting evaporation. The above results have shown that turbulence is a strong control parameter for dense clusters but it is not a control parameter for dilute clusters. This means that in order to influence evaporation in sprays one should install turbulence enhancement devices right at the exit of the atomizer where the spray is dense and not further down the length of the combustor where the spray has become dilute. Indeed it is well known empirically that this is true and the present results provide a theoretical justification for a well-known fact. However, it would be very desirable to have a set of experiments to compare with the predictions of the present theory. The present conclusions show that most of the sensitivity of our model and thus most of the control in an experiment can be expected in the dense-cluster regime. This makes a comparison so much more difficult because it is precisely in this regime that experiments are most difficult to perform because of the lack of resolution.

Acknowledgements—The research described in this paper was performed by the Jet Propulsion Laboratory, California Institute of Technology, and was supported by the Air Force Office of Scientific Research, Directorate of Aerospace Sciences; the Army Research Office, Engineering Sciences Division, and the U.S. Department of Energy, Office of Energy Utilization Research, Energy Conversion and Utilization Technologies Program, through interagencies agreements with the National Aeronautics and Space Administration.

REFERENCES

1. N. A. Chigier, C. P. Mao and V. Oechsle, Structure of air-assist atomizer spray, Paper 7-6A, CSS/WSS/Combustion Institute Spring Meeting, April (1985); also private communication.
2. J. Bellan and K. Harstad, The details of the convective evaporation of dense and dilute clusters of drops, *Int. J. Heat Mass Transfer* **30,** 1083–1093 (1987).
3. J. Bellan and K. Harstad, Analysis of the convective evaporation of non dilute clusters of drops, *Int. J. Heat Mass Transfer* **30,** 125–136 (1987).
4. J. Bellan and R. Cuffel, A theory of non dilute spray evaporation based upon multiple drop interactions, *Combustion Flame* **51,** 55–67 (1983).
5. G. M. Hidy and J. R. Brock, *The Dynamics of Aerocolloidal Systems*, pp. 99–101. Pergamon Press, Oxford (1970).
6. E. R. C. Eckert and R. M. Drake, Jr., *Heat and Mass Transfer*. McGraw-Hill, New York (1959).
7. C. Kittel, *Introduction to Solid State Physics*, 3rd Edn. Wiley, New York (1966).

APPENDIX

As explained in Section 3 θ_1 is obtained as a function of z from the conduction equation. The ten equations that are solved for the ten dependent variables identified at the end of Section 2 are as shown below. Define

$$g(\theta_{ga}, \theta_{gs}, Y_{Fva}, Y_{Fvs}, R_2, R_1) = \int_{R_1}^{R_2} \frac{y^2\,dy}{\theta_g(\sigma Y_{Fv}+\gamma)} \quad \text{(A1)}$$

$$f(\theta_{ga}, \theta_{gs}, Y_{Fva}, Y_{Fvs}, R_2, R_1) = \int_{R_1}^{R_2} \frac{y^2 Y_{Fv}\,dy}{\theta_g(\sigma Y_{Fv}+\gamma)} \quad \text{(A2)}$$

$$h(Y_{Fva}, Y_{Fvs}, R_2, R_1) = \int_{R_1}^{R_2} \frac{y^2\,dy}{\sigma Y_{Fv}+\gamma} \quad \text{(A3)}$$

where the integrations are performed using θ_g and Y_{Fv} as given by the approximation of equation (5).

The equations solved are as follows:

(1) $$\varepsilon = 1 - R_1^3 \quad \text{(A4)}$$

(2) $$C = -\alpha R_1^2 \frac{R^0}{4\pi(\rho_g D)^\infty}\left\{(1\text{ atm})\exp\left[\frac{C_{pg}w_F}{R_u}\left(\frac{1}{\theta_{bn}}-\frac{1}{\theta_{gs}}\right) + \frac{\Delta C_p w_F}{R_u}\left(1-\frac{\theta_{bn}}{\theta_{gs}}+\ln\frac{\theta_{bn}}{\theta_{gs}}\right)\right] - Y_{Fvs}\frac{p^\infty}{\sigma Y_{Fvs}+\gamma}\right\} \times \left(\frac{w_F C_{pg}}{2\pi R_u L_{bn}}\frac{1}{\theta_{gs}}\right)^{1/2} \quad \text{(A5)}$$

(3) $$R_1 = \left[1+3\frac{(\rho_g D)^\infty}{\rho_l R^{0^2}}\int_0^t C\,dt\right]^{1/3} \quad \text{(A6)}$$

(4) $$C = \frac{1}{-Z(R_1)}\ln\left\{1+\frac{\theta_{ga}-\theta_{gs}}{\frac{L}{L_{bn}}\frac{R_1}{C}\frac{\lambda_l}{C_{pg}(\rho_g D)^\infty}\frac{\partial\theta_l}{\partial z}\Big|_{z=1}}\right\} \quad \text{(A7)}$$

(5) $$Y_{Fvs} = 1+(Y_{Fva}-1)\exp(CZ(R_1)) \quad \text{(A8)}$$

(6) $$m_d\frac{du_d}{dt} = -\frac{1}{2}\left[N\rho_g A_d C_D u_r^2 + \frac{3\times 0.74}{4\pi R_2^3}\frac{m_d}{R^{0^3}}Wu_g u_d C_{Dc}A_c/N\right] \quad \text{(A9)}$$

(7) $$\frac{du_r}{dt} = -\frac{3\times 0.74}{4\pi R_2^3}\frac{1}{R^{0^3}} \times \left\{\dot{m}u_r/\rho_g + \frac{1}{2}\left[1+\frac{4\pi R_2^3}{3\times 0.74}\frac{R^{0^3}\rho_g N}{m_d}\right]A_d C_D u_r^2\right\} \quad \text{(A10)}$$

$$(8)\quad \frac{d\hat{m}_g}{d\tau} = -NC\frac{\hat{m}_g}{\hat{m}_g+\hat{m}_d} + N\frac{\hat{m}_d}{\hat{m}_g+\hat{m}_d}\frac{1}{\hat{\rho}_g^\infty}\frac{1}{\theta_{ga}(\sigma T_{Fva}+\gamma)} \times R_2^2\frac{dR_2}{d\tau} + \frac{u_r A_c}{4\pi R^0 D^\infty}\left[1-\frac{1}{\hat{\rho}_g^\infty}\frac{1}{\theta_{ga}(\sigma Y_{Fva}+\gamma)}\right] \quad (A11)$$

where

$$\hat{m}_g = \frac{N}{\hat{\rho}_g^\infty}\left[g(\theta_{ga},\theta_{gs},Y_{Fvs},Y_{Fva},R_2,R_1) + \frac{1-0.74}{0.74}\frac{R_2^3}{3}\frac{1}{\theta_{ga}(\sigma Y_{Fva}+\gamma)}\right] \quad (A12)$$

$$(9)\quad \frac{d\hat{m}_{Fv}}{d\tau} = -NC\left(1-Y_{Fva}\frac{\hat{m}_d}{\hat{m}_g+\hat{m}_d}\right) + \frac{M_{F2,j}}{4\pi(\rho_g D)^\infty R^0} + \frac{u_r A_c}{4\pi D^\infty R^0}\left[Y_{Fv}^\infty - \frac{1}{\hat{\rho}_g^\infty}\frac{Y_{Fva}}{\theta_{ga}(\sigma Y_{Fva}+\gamma)}\right] + \frac{N}{\hat{\rho}_g^\infty}\frac{Y_{Fva}}{\theta_{ga}(\sigma Y_{Fva}+\gamma)}\frac{\hat{m}_d}{\hat{m}_g+\hat{m}_d}R_2^2\frac{dR_2}{d\tau} \quad (A13)$$

where

$$\hat{m}_{Fv} = \frac{N}{\hat{\rho}_g^\infty}\left[f(\theta_{ga},\theta_{gs},Y_{Fva},Y_{Fvs},R_2,R_1) + \frac{1-0.74}{0.74}\frac{R_2^3}{3}\frac{Y_{Fva}}{\theta_{ga}(\sigma Y_{Fva}+\gamma)}\right] \quad (A14)$$

$$(10)\quad \frac{d\hat{H}}{d\tau} = \frac{u_r A_c}{4\pi R^0 D^\infty}\left[\frac{h^G}{L_{bn}} + \theta_g^\infty - 1 + \frac{\dfrac{h^G}{L_{bn}}+\theta_{ga}-1}{\hat{\rho}_g^\infty\theta_{ga}(\sigma Y_{Fva}+\gamma)}\right] + \frac{E_{2,j}}{4\pi R^0 L_{bn}(\rho_g D)^\infty} + N\frac{\hat{m}_d}{\hat{m}_g+\hat{m}_d}\left(\frac{h^G}{L_{bn}}+\theta_{ga}-1\right) \times\left[C+\frac{1}{\theta_{ga}(\sigma Y_{Fva}+\gamma)\hat{\rho}_g^\infty}R_2^2\frac{dR_2}{d\tau}\right] \quad (A15)$$

where

$$\frac{R_u^*}{p^\infty w_F C_{pg} 4\pi R^{0^3}}NH = \hat{\rho}_l\left[\frac{R_1^3}{3}\frac{h^L}{L_{bn}} + \frac{C_{pl}}{C_{pg}}\int_0^{R_1}(\theta_l-1)y^2\,dy\right] + \left(\frac{h^G}{L_{bn}}-1\right)g(\theta_{ga},\theta_{gs},Y_{Fvs},Y_{Fva},R_2,R_1) + h(Y_{Fva},Y_{Fvs},R_2,R_1) + \frac{1-0.74}{0.74}\frac{R_2^3}{3}\frac{h^G/L_{bn}+\theta_{ga}-1}{\theta_{ga}(\sigma Y_{Fva}+\gamma)}. \quad (A16)$$

EFFETS DE LA TURBULENCE PENDANT L'EVAPORATION DE GOUTTES DANS DES GRAPPES

Résumé—On présente un modèle d'évaporation de gouttelette dans des grappes et les mécanismes d'échange entre la grappe et la phase gazeuse environnante. Ce modèle est développé pour utiliser un modèle de sous-échelle dans les calculs d'évaporation et de combustion d'aérosols et pour décrire le comportement global de la grappe, la pression du gaz demeure constante pendant l'évaporation et par suite le volume de la grappe et la densité du nombre de gouttes varient. On considère deux modèles de turbulence; le premier décrit l'évaporation dans l'environnement initialement sans turbulence laquelle se constitue au cours du temps; le second modèle décrit l'évaporation dans l'environnement lorsque la turbulence existe initialement. Les résultats obtenus montrent que la turbulence augmente l'évaporation et qu'elle est un facteur de commande de l'évaporation des grappes très denses. Lorsque le rapport initial des masses air/combustible augmente, à la fois l'histoire de la turbulence et la vitesse relative initiale entre gouttes et gaz peuvent contrôler l'évaporation. On montre que le temps d'évaporation diminue avec un accroissement initial des niveaux de turbulence ou de la vitesse relative. Lorsque le rapport initial des masses air/combustible augmente encore plus et que la densité initiale du nombre de gouttes entre le régime de dilution, aucun des deux paramètres ne peut contrôler l'évaporation. Le temps d'évaporation décroît avec la diminution de la taille de la grappe pour des grappes de gouttes denses, tandis que la taille de la grappe n'est pas un facteur limitant pour les grappes diluées. On discute des implications pratiques de ces résultats.

EINFLUSS DER TURBULENZ AUF DIE VERDAMPFUNG VON TROPFEN IN SCHWÄRMEN

Zusammenfassung—Ein Modell für die Tropfenverdampfung in Schwärmen und für die Austauschprozesse zwischen dem Schwarm und der umgebenden Gasphase wird vorgestellt. Dieses Modell wurde zur Berechnung der Sprühverdampfung und der Verbrennung entwickelt und beschreibt nur globale Verhaltensmerkmale von Tropfenschwärmen. Der Gasdruck im Tropfenschwarm bleibt während der Verdampfung konstant, als Folge davon variiert das Volumen des Tropfenschwarms und die Tropfenanzahl pro Volumeneinheit. Zwei Turbulenzmodelle werden herangezogen. Das erste Modell beschreibt die Verdampfung von Tropfenschwärmen in einer Umgebung, die anfänglich turbulenzfrei ist; die Turbulenz baut sich erst mit der Zeit auf. Das zweite Modell beschreibt die Verdampfung von Tropfenschwärmen in einer Umgebung, in der von Anfang an Turbulenz vorliegt. Die mit diesen Modellen erhaltenen Ergebnisse zeigen, daß Turbulenz die Verdampfung begünstigt und ein kontrollierender Parameter bei der Verdampfung von sehr dichten Tropfenschwärmen ist. Beispiele werden gezeigt, in denen mit dem ersten Turbulenzmodell Sättigung vor der vollständigen Verdampfung erhalten wurde, wogegen sich mit dem zweiten Turbulenzmodell das Gegenteil ergab. Steigt das Anfangs-Massenverhältnis Luft/Brennstoff, so kann sowohl die Vorgeschichte der Turbulenz als auch die Anfangs-Relativgeschwindigkeit zwischen Tropfen und Gas die Verdampfung beeinflussen. Es wird gezeigt, daß die Verdampfungszeit mit einer Erhöhung des Turbulenzgrades oder der Anfangs-Relativgeschwindigkeit abnimmt. Steigt das Anfangs-Massenverhältnis Luft/Brennstoff weiter und fällt die Tropfenanzahl pro Volumeneinheit zu Beginn in den Bereich für lockere Schwärme, so beeinflußt keiner der beiden obengenannten Parameter die Verdampfung. Bei dichten Tropfenschwärmen verkürzt sich die Verdampfungszeit mit abnehmender Größe des Schwarms; bei lockeren Schwärmen hat die Größe keinen Einfluß. Die praktischen Folgerungen aus den Ergebnissen werden diskutiert.

ЭФФЕКТЫ ТУРБУЛЕНТНОСТИ ПРИ ИСПАРЕНИИ КЛАСТЕРОВ КАПЕЛЬ

Аннотация—Представлена модель испарения кластеров капель и описаны процессы обмена между кластерами и несущей газовой средой. Разработанная модель, являясь подсеточной, используется для расчета испарения и горения распылов капель, а поэтому учитывает только глобальные особенности поведения испаряющихся кластеров. Предполагается, что в процессе испарения давление газа в кластере остается постоянным, так что переменными являются объем кластера и плотность числа капель в нем. Рассмотрены две модели турбулентности. Первая описывает испарение кластера в среде, в которой вначале турбулентность отсутствует, но "подключается" со временем по мере испарения кластеров. Вторая модель описывает испарение кластера в среде с начальной турбулентностью. Согласно обеим моделям турбулентность ускоряет испарение, являясь определяющим фактором при испарении очень плотных кластеров. Приведены примеры, в которых показано, что с использованием первой модели насыщение наступает до полного испарения капель, а с использованием второй наблюдается противоположный эффект. При увеличении начального массового отношения воздух/горючее испарение зависит как от предыстории турбулентности, так и от начальной относительной скорости движения капель и газа. Показано, что время испарения уменьшается, если начальный уровень турбулентности или относительная скорость возрастают. При существенном увеличении начального массового отношения воздух/топливо и уменьшении начальной плотности числа капель до разреженного режима ни один из вышеуказанных параметров не оказывает решающего влияния на испарение. Кроме того показано, что время испарения уменьшается с уменьшением размера кластера при большой плотности числа капель, а при малой плотности размер кластера не является определяющим фактором. Обсуждаются практические аспекты полученных результатов.